

Supporting Information

Guedj et al. 10.1073/pnas.1203110110

SI Methods

Data Fitting and Statistical Methods. Patient viral load data were fit using nonlinear mixed-effect models, which borrow strength from the whole sample to estimate more precisely the population parameters, such as the mean, and the interindividual variation (IIV) (1). In this approach, each parameter θ_i comprises a fixed part θ , which represents the median value of the parameter in the population, and a random part η_i chosen from a Gaussian distribution with mean 0 and SD equal to IIV that accounts for the IIV. Parameters are log-transformed to ensure positivity, and we write $\theta_j = \theta \cdot e^{\eta_j}$. We used a logistic transformation of the ε_j 's ($j = s, \alpha$) to ensure that the antiviral treatment effectiveness is between 0 and 1, and we write $\varepsilon_{ji} = \frac{\varepsilon_j}{\varepsilon_j + (1 - \varepsilon_j)e^{\eta_j}}$.

Data were analyzed using MONOLIX (www.lixoft.com), a software devoted to maximum likelihood estimation of parameters in nonlinear mixed-effect models (2). After the population parameters were found, the values of the parameters for individual patients were deduced using empirical Bayes estimates (3).

Cells and Virus. Huh7-1 cells were described previously (4). Cells were passaged in complete DMEM (HyClone) supplemented with 10% (vol/vol) FBS (HyClone), 100 U/mL penicillin, 100 mg/mL streptomycin, and 2 mM L-glutamine (Gibco Invitrogen). JFH-1 cell culture-propagated HCV (HCVcc) viral stocks were obtained by infection of naive Huh7-1 cells at a multiplicity of infection (MOI) of 0.01 focus-forming units (FFU) per cell, using medium from Huh7-1 cells electroporated with in vitro-transcribed full-length infectious HCV JFH-1 RNA generated from pJFH-1 provided by Takaji Wakita (National Institute of Infectious Diseases, Tokyo, Japan) as described previously (5).

HCVcc Inhibition Experiments. Huh7 cells were seeded in 96-well BioCoat culture plates at a density of 8×10^3 cells per well in complete DMEM (cDMEM). Upon reaching 90–95% confluence, medium was replaced with 200 μ L cDMEM supplemented with 1% DMSO (Sigma), and cells were cultured for an additional 20 d, replacing medium every 2 d. These cultures are referred to as DMSO-Huh7 cells and were described and characterized previously (5–7). For HCV infection experiments, DMSO-Huh7 cultures were inoculated with HCVcc JFH-1 at an MOI of 0.05 FFU per cell and cultured for an additional 10 d to allow HCV levels to reach steady state. Parallel cultures of steady-state HCV-infected cells were then either mock treated or treated with 25 μ M NM107

or 1 nM daclatasvir. At indicated times, medium was harvested from eight replicate wells for titer analysis and cell lysate was harvested in 200 μ L 1 \times Nucleic Acid Purification Lysis Solution (Applied Biosystems) from four replicate wells for isolation of RNA. Real-time quantitative PCR (RTqPCR) analysis for HCV RNA and cellular GAPDH mRNA was performed as described below.

RNA Isolation and RTqPCR Analysis. Total cellular RNA was purified using an ABI PRISM 6100 Nucleic Acid Prep Station (Applied Biosystems) according to the manufacturer's instructions. Reverse transcription and RTqPCR were performed using TaqMan reverse transcription reagents (Applied Biosystems) and FastStart Universal SYBR Green Master mix (Roche), respectively, and using the following primers: universal HCV primers (8) 5'-GCC TAG CCA TGG CGT TAG TA -3' (sense) and 5'-CTC CCG GGG CACTCG CAA GC-3' (antisense) and human GAPDH (9) 5'-GAA GGT GAA GGT CGG AGT C-3' (sense) and 5'-GAA GAT GGT GAT GGG ATT TC-3' (antisense). HCV RNA copies were determined relative to a standard curve composed of serial dilutions of a plasmid containing the JFH-1 HCV cDNA (pJFH-1).

Extracellular Infectivity Titration Assay. Cell supernatants were serially diluted 10-fold in cDMEM, and 200 μ L per well was used to infect quadruplicate Huh7 cultures in 96-well plates (BD Biosciences). Because NM107- and daclatasvir-treated samples contained potentially inhibitory drugs, the same concentration of each drug was added to two of the four mock-treated samples before serial dilution. The drug-containing virus/medium sample was then removed at 8 h post inoculation, cells were washed so that the titer assay could proceed in the absence of the antiviral compounds, and monolayers were overlaid with DMEM containing 0.25% methylcellulose (wt/vol) (Fluka BioChemika). As a control to monitor for possible inhibitor effects of the compounds, representative mock samples also were titered in the absence of any drug addition. At 72 h post inoculation, medium was removed, cells were fixed with 4% paraformaldehyde (Sigma), and immunohistochemical staining for HCV E2 was performed as described previously (10). Viral infectivity titers are expressed as FFU per milliliter of supernatant, determined by the average number of E2-positive foci detected in quadruplicate samples at the highest HCV-positive dilution.

1. Guedj J, Thiébaud R, Commenges D (2007) Maximum likelihood estimation in dynamical models of HIV. *Biometrics* 63(4):1198–1206.
2. Kuhn E, Lavielle M (2005) Maximum likelihood estimation in nonlinear mixed effects models. *Comput Stat Data Anal* 49(4):1020–1038.
3. Pinheiro J, Bates D (2000) *Mixed-Effects Models in S and S-PLUS* (Springer, New York).
4. Sainz B, Jr., Barretto N, Uprichard SL (2009) Hepatitis C virus infection in phenotypically distinct Huh7 cell lines. *PLoS ONE* 4(8):e6561.
5. Yu X, Uprichard SL (2010) Cell-based hepatitis C virus infection fluorescence resonance energy transfer (FRET) assay for antiviral compound screening. *Curr Protoc Microbiol*, Chapter 17:Unit 17.15.
6. Sainz B, Jr., Chisari FV (2006) Production of infectious hepatitis C virus by well-differentiated, growth-arrested human hepatoma-derived cells. *J Virol* 80(20):10253–10257.
7. Choi S, Sainz B, Jr., Corcoran P, Uprichard SL, Jeong H (2009) Characterization of increased drug metabolism activity in dimethyl sulfoxide (DMSO)-treated Huh7 hepatoma cells. *Xenobiotica* 39(3):205–217.
8. Komurian-Pradel F, et al. (2004) Strand specific quantitative real-time PCR to study replication of hepatitis C virus genome. *J Virol Methods* 116(1):103–106.
9. Zhong J, et al. (2005) Robust hepatitis C virus infection in vitro. *Proc Natl Acad Sci USA* 102(26):9294–9299.
10. Yu X, Sainz B, Jr., Uprichard SL (2009) Development of a cell-based hepatitis C virus infection fluorescent resonance energy transfer assay for high-throughput antiviral compound screening. *Antimicrob Agents Chemother* 53(10):4311–4319.

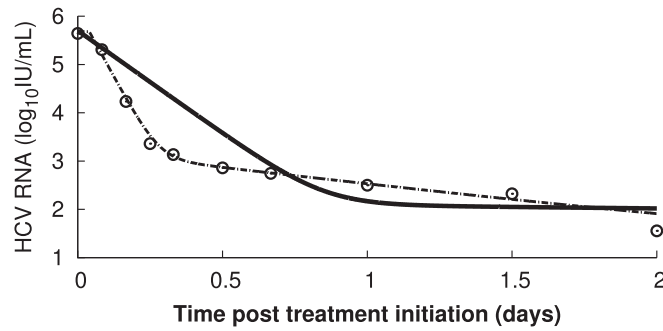


Fig. 54. Viral load decline in a patient treated with daclatasvir (Pt 8, \circ) and the corresponding best-fit model prediction (solid line) using the multiscale model (Eq. 3), assuming daclatasvir blocks only viral RNA (vRNA) replication and has no effect on virion assembly/secretion (i.e., $\varepsilon_s = 0$). Estimated parameters are $V_0 = 5.64 \log_{10}$ IU/mL, $t_0 = 0$, $c = 200 \text{ d}^{-1}$, and $\varepsilon_\alpha = 0.99989$. Other parameters are fixed to values given in Table 2. Dashed line is the best-fit prediction assuming daclatasvir blocks both vRNA replication and assembly/secretion (parameters are given in Table S3).

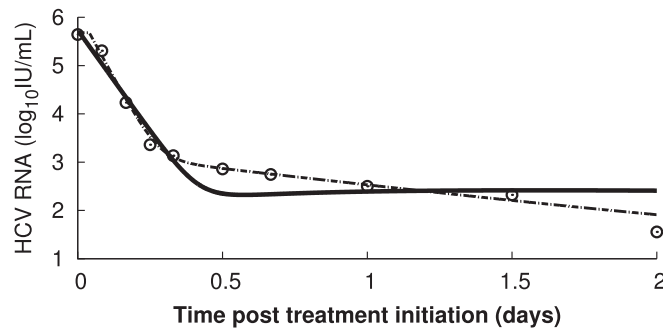


Fig. 55. Viral load decline in a patient treated with daclatasvir (Pt 8, \circ) and the corresponding best-fit model prediction using the multiscale model, assuming daclatasvir blocks only viral assembly/secretion and has no effect on vRNA replication (i.e., $\varepsilon_\alpha = 0$). Estimated parameters are $V_0 = 5.64 \log_{10}$ IU/mL, $t_0 = 0$, $c = 19 \text{ d}^{-1}$, and $\varepsilon_s = 0.99997$. Other parameters are fixed to values given in Table 2. Dashed line is the best-fit prediction assuming daclatasvir blocks both vRNA replication and assembly/secretion (parameters are given in Table S3).

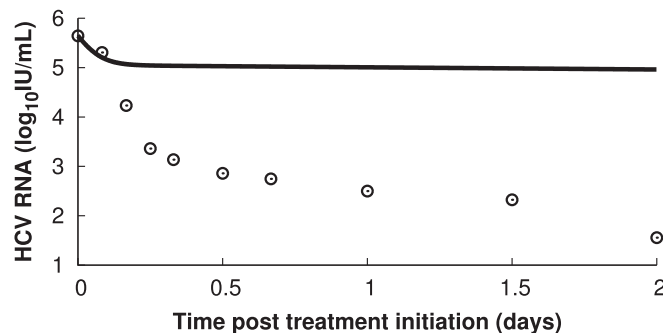


Fig. 56. Multiscale model prediction (solid line) assuming that daclatasvir increases only the virion clearance rate, c , fourfold. Parameters are as given in Table 2, except $\varepsilon_\alpha = 0$, $\varepsilon_s = 0$, and c is increased from 5.625 d^{-1} to 22.5 d^{-1} , i.e., fourfold at $t = 0$. Note that increasing the clearance rate alone does not lead to predictions consistent with patient data (Pt 8, \circ).

Table S1. Population parameter estimates for patients treated with daclatasvir for different values of α and δ

δ	α															
	10				20				40				100			
	$\kappa\mu$	c	ε_s	ε_α	$\kappa\mu$	c	ε_s	ε_α	$\kappa\mu$	c	ε_s	ε_α	$\kappa\mu$	c	ε_s	ε_α
0.01	1.63	22.3	0.998	0.99	1.6	22.3	0.998	0.991	1.52	22.2	0.998	0.992	1.56	22.5	0.998	0.992
0.14	1.51	22.2	0.998	0.99	1.51	22.3	0.998	0.99	1.46	22.3	0.998	0.99	1.6	22.4	0.998	0.99
0.58	1.35	22.5	0.998	0.97	1.14	22.1	0.998	0.98	1.13	22.4	0.998	0.98	1.14	22	0.998	0.98

Default values used in the main analysis are $\alpha = 40 \text{ d}^{-1}$ and $\delta = 0.14 \text{ d}^{-1}$.

Table S2. Population parameter estimates obtained using the approximate solution (Eq. 3) of the multiscale model including data from nine patients treated with 1,250 mg TVR twice daily

δ (d^{-1})	ε_{α}				ε_s			ρ (d^{-1})	c (d^{-1})	$\kappa\mu$ (d^{-1})	
	IFN, 5 MIU	IFN, 10/15 MIU	Daclatasvir	TVR	IFN, 5/10/15 MIU	Daclatasvir	TVR			IFN/daclatasvir*	TVR
0.01	0.79	0.97	0.98	0.99	0.36	0.997	0.95	6.32	22.6	1.77	3.97
0.14	0.76	0.96	0.98	0.99	0.44	0.997	0.94	7.46	22.7	1.68	3.85
0.58	0.66	0.94	0.97	0.98	0.33	0.998	0.93	8.16	23.2	1.67	4.05

MIU, million international units.

*We found that $\kappa\mu$ is identical under IFN and daclatasvir monotherapy.

Table S3. Empirical Bayes estimates of individual parameter in the multiscale model

Treatment	Pt	ε_{α}	ρ	V_0	t_0	ε_s	$\kappa\mu$	c
IFN, 5 MIU	1A	0.67	7.88	6.65	0.46	0.33	1.46	22.27
	1B	0.78	8.95	6.37	0.37	0.37	1.46	22.42
	1E	0.91	9.26	6.03	0.43	0.31	1.46	22.35
	1F	0.80	7.36	6.87	0.50	0.34	1.46	22.22
	1H	0.63	8.44	6.68	0.42	0.77	1.46	22.41
	1Q	0.78	8.95	6.37	0.37	0.37	1.46	22.42
Mean		0.76	8.47	6.49	0.43	0.41	1.46	22.35
IFN, 10/15 MIU	2A	0.80	7.67	6.78	0.47	0.34	1.46	22.26
	2B	0.97	8.63	7.17	0.47	0.32	1.46	22.29
	2C	0.94	8.76	6.64	0.45	0.32	1.46	22.32
	2D	0.90	8.95	6.00	0.40	0.79	1.46	22.97
	2E	0.995	12.65	7.55	0.39	0.23	1.46	22.33
	2F	0.93	8.14	6.93	0.35	0.40	1.46	22.42
	2G	0.88	6.95	7.37	0.36	0.52	1.46	22.35
	2H	0.99	9.43	6.39	0.38	0.28	1.46	22.27
	3A	0.99	5.46	6.81	0.48	0.56	1.46	22.26
	3B	0.93	7.75	6.59	0.40	0.81	1.46	22.85
	3C	0.97	7.80	6.67	0.81	0.28	1.46	22.08
	3D	0.99	8.29	5.59	0.30	0.82	1.46	22.90
3E	0.93	9.36	7.24	0.34	0.35	1.46	22.48	
3F	0.88	7.06	6.05	0.56	0.32	1.46	22.16	
Mean		0.94	8.35	6.70	0.44	0.45	1.46	22.42
Daclatasvir	8	0.997	7.39	5.68	0.04	0.997	1.46	25.44
	42	0.97	9.17	5.57	0.03	0.997	1.46	23.12
	68	0.99	8.02	7.24	0.05	0.998	1.46	20.10
	69	0.98	8.75	6.15	0.04	0.999	1.46	22.74
	83	0.99	8.19	5.67	0.05	0.997	1.46	20.46
Mean		0.98	8.30	6.06	0.04	0.998	1.46	22.37